· Article · Advances in Polar Science
doi: 10.13679/j.advps.2017.3.00196 September 2017 Vol. 28 No. 3: 196–203

Sea ice classification in the Weddell Sea based on scatterometer data

GAO Xiang[1], PANG Xiaoping[1,2] & JI Qing[1,3*]

[1] Chinese Antarctic Center of Surveying and Mapping, Wuhan University, Wuhan 430079, China;
[2] Collaborative Innovation Center for Territorial Sovereignty and Maritime Rights, Wuhan University, Wuhan 430072, China;
[3] Key Laboratory of Polar Surveying and Mapping, National Administration of Surveying, Mapping and Geoinformation, Wuhan 430079, China

Received 6 March 2017; accepted 27 July 2017

Abstract Sea ice type is an important factor for accurately calculating sea ice parameters such as sea ice concentration, sea ice area and sea ice thickness using satellite remote sensing data. In this study, sea ice in the Weddell Sea was classified from scatterometer data by the histogram threshold method and the Spreen model method, and evaluated and validated with the Antarctic Sea Ice Processes and Climate (ASPeCt) sea ice type ship-based observations. The results show that the two methods can both distinguish multi-year (MY) ice and first-year (FY) ice during the ice growth season, and that the histogram threshold method has a relatively larger MY ice classification extent than the Spreen model. The classification accuracy of the histogram threshold method is 77.8%, while the Spreen model method accuracy is 80.3% compared with the ship-based observations, thus indicating that the Spreen model method is better for discriminating MY ice from FY ice from scatterometer data. These results provide a basis and reference for further retrieval of long-time sea ice type information for the whole Antarctica.

Keywords **sea ice type, QuikSCAT, ASPeCt, Weddell Sea**

Citation: Gao X, Pang X P, Ji Q. Sea ice classification in the Weddell Sea based on scatterometer data. Adv Polar Sci, 2017, 28(3): 196–203, doi: 10.13679/j.advps.2017.3.00196

1 Introduction

The Antarctic is a key area sensitive to climate change (Ma et al., 2004), and sea ice there plays an important role in the climate system, affecting both regional and global climate changes (Heygster and Wang, 2010; Zwally et al., 2002). To assess the impact of sea ice on climate change, sea ice parameters are required such as sea ice concentration and sea ice thickness. Estimation of sea ice thickness is dependent on sea ice type (Thomdike et al., 1975). Therefore, it is important to obtain accurate sea ice type information for the study of sea ice and climate change.

Recently, distinguishing multi-year (MY) sea ice from first-year (FY) sea ice on a large scale using remote sensing data has been a contentious issue in sea ice research. Gloersen and Cavalieri used the polarization ratio (PR) derived from passive microwave brightness temperature data to identify seawater and sea ice, and then applied the Spectral Gradient Ratio (GR) threshold to distinguish between FY ice and MY ice in the Arctic (Gloersen and Cavalieri, 1986). In their study, the relationship between GR and PR was plotted, and the GR threshold of 0.02 was found to distinguish MY ice. Maslanik et al. (2011). used the Lagrangian operator to compute the ice age distribution of Arctic sea ice based on passive microwave remote sensing data. Ice age was estimated by treating each grid cell that contains ice as a discrete, independent Lagrangian parcel, and then transporting the parcels at weekly time

* Corresponding author, E-mail: jiqing@whu.edu.cn

steps. Geldsetzer and Yackel (2009) identified Arctic FY ice and MY ice using dual-polarized C-band Synthetic Aperture Radar (SAR) images. In their study, a decision-tree classifier was presented using estimated statistical thresholds based on the analysis of thin sea ice, FY ice, MY ice and open water in the Canadian Arctic during the winter. Walker et al. (2006) classified Arctic sea ice jointly using scatterometer and passive microwave remote sensing data, with the analysis method using a passive microwave signature and a scatterometer signature. In the Antarctic, Ozsoy-Cicek et al. (2011) made an intercomparison between Radarsat-1 SAR, Envisat ASAR, QuikSCAT and AMSR-E snow depth. These formed two clearly separated clusters, one for 0.24–0.35 m depth (on FY ice) and one for 0.36–0.54 m depth (on MY ice) (Ozsoy-Cicek et al., 2011). Lythe et al. (1999) combined ERS-2 SAR and Advanced Very High Resolution Radiometer (AVHRR) data to distinguish six sea ice types in the Ross Sea using a segmentation algorithm based on the iterative application of the Gamma-Map speckle reduction filter.

Nevertheless, previous studies on the large-scale classification of sea ice have mainly focused on the Arctic. In these, the main types of data used have been passive microwave radiometer (25 km resolution), SAR (100 m) and scatterometer (about 20 km). The passive microwave remote sensing data cover a large area, but the spatial resolution is relatively low, and the SAR image with high spatial resolution cannot be used to obtain sea ice type information on a large-scale. The enhanced-resolution scatterometer data accessed from the Brigham Young University Center for Remote Sensing has a higher spatial resolution (2.225 km) than the passive microwave data and a larger coverage than SAR images, and thus is an ideal data source for obtaining large-scale sea ice type information.

The scatterometer backscatter of sea ice is influenced by salinity and surface roughness, which determine dielectric properties. The simulated mean salinity of sea ice in the Arctic and Antarctic is 3.6‰ and 6.3‰, respectively (Vancoppenolle et al., 2009). The sea ice salinity is higher in the Antarctic because of the higher relative contribution of young ice. The root-mean-square (RMS) roughness of sea ice measured during a transect of the Weddell Sea is ranged from 0.1 to 1.1 m (Andreas et al., 1993), and the value for Arctic sea ice ranged from 0.09 to 0.21 m (Beckers et al., 2015). The physical properties of Arctic and Antarctic sea ice have similarities, making it possible to apply Arctic sea ice classification methods to the Antarctic.

The two principal methods for classifying sea ice from scatterometer data are the histogram threshold method (Kwok, 2004) and the Spreen model method (Spreen, 2008). In this paper, we tested these two different sea ice classification methods in the Weddell Sea using QuikSCAT scatterometer data, and validated the result against ship-based observational data. The aim of the study is to compare and assess sea ice classification methods in order to better understand their relative performance using scatterometer remote sensing data, so as to retrieve long-term Antarctic sea ice type information in the future.

2 Data and methods

2.1 Study area

The region of this study is the Weddell Sea (Figure 1), which is between 60°W, 20°E, and around the Antarctic continent, including the East Weddell Sea and West Weddell Sea. In Antarctic, there is a larger area of sea ice, especially of MY ice, in the Weddell Sea than in other regions. In general, the area of sea ice reaches a maximum in September and a minimum in February.

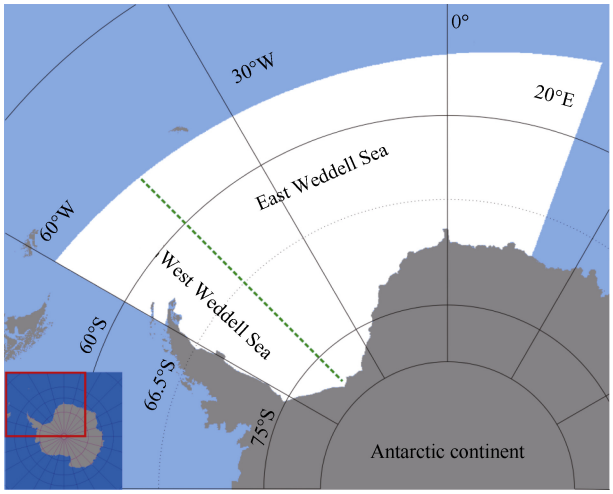

Figure 1 Schematic of the study area. The white shading denotes the extent of the Weddell Sea, the green dotted line, longitude 45°W, separates the East Weddell Sea and the West Weddell Sea.

2.2 Data

2.2.1 QuikSCAT scatterometer data

QuikSCAT is a sun-synchronous orbit satellite with an orbital altitude of 803 km and an inclination angle of 98.6 degrees. The instrument aboard QuikSCAT is the SeaWinds scatterometer, which is identically named to the scatterometer aboard the Advanced Earth Observation Satellite 2 (ADEOS-II). To distinguish the two instruments, NASA Jet Propulsion Laboratory (NASA/JPL) renamed the SeaWinds instrument aboard the QuikSCAT satellite to QuikSCAT. The QuikSCAT scatterometer operates at a Ku-band frequency of 13.4 GHz using the internal and external beam scanning modes. The horizontally polarized (HH) inner beam covers 1400 km at an incidence angle of 46 degrees, and the vertically polarized (VV) outer beam covers a range of 1800 km at an incidence angle of 54 degrees. The QuikSCAT covers 90% of the Earth's surface in one day, and is designed to measure the wind speed and direction over the ocean, as well as to monitor sea ice (NSA/JPL, 2006).

In this paper, the QuikSCAT scatterometer data, with the spatial resolution of 2.225 km and the temporal resolution of one day, were downloaded from Brigham Young University (http://www.scp.byu.edu/data/SigBrw/SigBrw.html). The enhanced resolution QuikSCAT scatterometer data, which take advantage of the spatial overlap in scatterometer measurements made at different times of day, can provide more detail of the sea ice compared to the original resolution (Early and Long, 2001; Long et al., 1993). Following the previous study (Spreen, 2008), the data we used in this study for distinguishing MY ice and FY ice are the vertical polarized (VV) scatterometer data.

2.2.2 AMSR-E sea ice concentration data

The Advanced Microwave Scanning Radiometer for Earth Observing System (AMSR-E) is a passive microwave radiometer aboard the NASA Aqua satellite, with an incident angle of 55 degrees and six frequencies with vertical polarization and horizontal polarization (Kawanishi et al., 2003). The radiation difference between sea ice and seawater at different frequencies, gradient ratio and polarization, from AMSR-E data are frequently used to compute the extent of sea ice. AMSR-E ASI daily sea ice concentration data used in this study were obtained from Bremen University (http://iup.physik.uni-bremen.de:8084/amsr/), with a spatial resolution of 6.25 km.

2.2.3 ASPeCt ship-based observational data

The Antarctic Sea Ice Processes and Climate (ASPeCt) dataset (http://aspect.antarctica.gov.au/data) is an archival collection of sea ice observations made during ice navigation on scientific expeditions. The dataset contains sea ice parameters including sea ice concentration, sea ice thickness and sea ice type, which are recorded on the ship within an observation distance of 1 km (Worby et al., 2008). After training, using the ASPeCt tutorial (which provides photographs and descriptions of different ice types) ice observers can record the sea ice type from vessels operating in the Antarctic. For the Antarctic, the ASPeCt dataset is available from 1984 to 2005. The observed data points coinciding with the QuikSCAT data in the Weddell Sea are shown in Figure 2, and we extracted the acquired sea ice type information from the ASPeCt dataset to validate sea ice classification results based on the scatterometer data.

2.3 Sea ice classification methods

The Southern Ocean is a typical seasonal (FY) ice zone, while MY ice also usually exists in the Weddell Sea. In this section, we first introduce the two classification methods, and then describe our workflow used for sea ice classification in this paper.

2.3.1 Histogram threshold method

MY ice contains much less brine and more air pockets than FY ice. Due to the large salinity and roughness difference between MY ice and FY ice, the scattering effect of MY ice is stronger than FY ice, resulting in a higher backscatter coefficient in the scatterometer image. These will lead to a peak-valley pattern in the histogram of scatterometer data (Kwok, 2004). Hence it is possible to set a threshold to separate MY ice and FY ice from the histogram of the scatterometer data. However, several different thresholds of the histogram have been reported. Kwok (2004) applied the scatterometer histogram with a threshold of –14.5 dB for classifying Arctic FY ice and MY ice, while Haarpaintner et al. (2006) used a threshold of –12 dB for the Arctic. As the physical properties of FY and MY ice change every day, including surface roughness, brine content, and ice thickness, they contribute to observed differences in backscatter (Tucker et al., 1991), and the error may be large if only a fixed threshold is used to classify FY ice and MY ice. Therefore, in this paper, we adopted a self-adaptive daily sea ice classification threshold according to the distribution of each histogram. The threshold, classifying the MY ice and FY ice, is set to the lowest value between two peaks with a constrained condition that the threshold should be in the range between –17 dB and –12 dB.

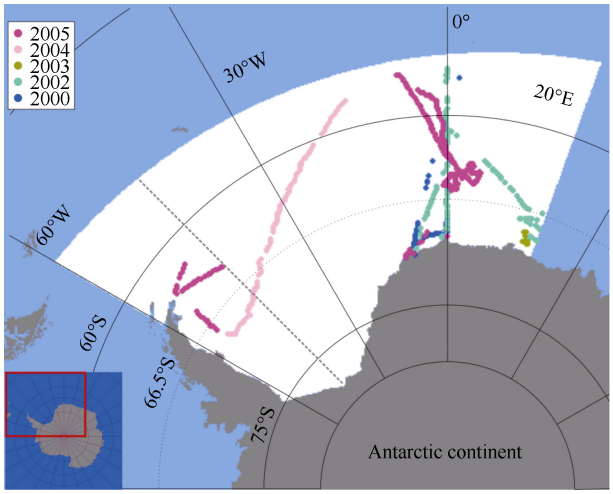

Figure 2 Positions of the ASPeCt measurement points in the study area. The color of the dots indicates the year of the scientific research cruise.

2.3.2 Spreen model method

The Spreen model is a sea ice classification model which based on the relationship between Radarsat remote sensing data and QuikSCAT scatterometer data (Spreen, 2008). MY ice fraction for three winter time months (December 1999 to February 2000) were derived from Radarsat data using the Radarsat geophysical processor system (Kwok, 1998). A seventh order polynomial, L_{MY}, was used to fit the relationship between C_{MYf} and QuikSCAT backscatter using a least-square method. Once the model of the relationship between MY ice concentration and QuikSCAT scatterometer data was built, MY ice concentration can be retrieved from QuikSCAT scatterometer data. The model can be expressed as in equation (1) and equation (2).

$$L_{MY}=45.4268+27.9618\sigma_{VV}+7.08118\sigma_{VV}^{2}+0.943513\sigma_{VV}^{3}+0.0720040\sigma_{VV}^{4}+0.00317470\sigma_{VV}^{5}+7.53719\times10^{-5}\sigma_{VV}^{6}+7.46839\times10^{-7}\sigma_{VV}^{7} \quad (1)$$

$$C_{MY}=\begin{cases}0, & \sigma_{VV}\leqslant -21dB\\ L_{MY}, & -21dB\leqslant\sigma_{VV}\leqslant -9dB\\ 1, & \sigma_{VV}\geqslant -9dB\end{cases} \quad (2)$$

Where, σ_{VV} refers to the vertical polarization backscatter coefficient of QuikSCAT, L_{MY} represents the component of MY ice whose value is between 0 and 1, and C_{MY} is the percentage of MY ice in one pixel.

2.3.3 Workflow of the data processing

Figure 3 shows the workflow of the data processing in this study. The QuikSCAT data of 2.225 km resolution was firstly resampled based on the Nearest Neighbor method to match the AMSR-E sea ice concentration product, and then sea ice extent was calculated noting that AMSR-E sea ice concentration is always greater than 15%. The sea ice zone of the Weddell Sea was extracted using a geographic mask of the area. Finally, we classified sea ice in the study area by the histogram threshold method and the Spreen model, compared the results against the sea ice type information extracted from ASPeCt ship-observation data.

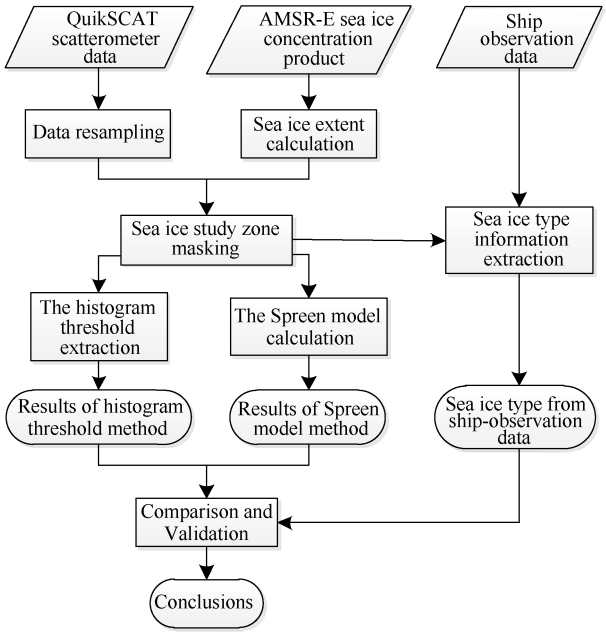

Figure 3 Workflow of the data processing.

3 Results and analysis

3.1 Histogram of QuikSCAT data in the Weddell Sea

The QuikSCAT scatterometer data of the 10th and 20th day of every month in 2005 were selected to make the histogram (Figure 4). The number of sea ice pixels shows an increasing trend from March to September when Weddell Sea ice was in the growth stage, and the opposite from October to February when Weddell Sea ice was in the melt season. In the growth stage of sea ice, there is an obvious peak-valley structure from the QuikSCAT scatterometer histogram, but a sea ice classification threshold is not evident during the melt season, which is consistent with the conclusion that Kwok made from the Arctic sea ice scatterometer histogram (Kwok, 2004).

3.2 Classification results of the histogram threshold method and the Spreen model method

As the time window of ASPeCt ship-based observational data for the Weddell Sea is from 30 July, 2005 to 7 September, 2005, QuikSCAT data of 31 July, 2005 and 19 August, 2005 were selected for the study. The typical classification results of 31 July and 19 August are shown in Figure 5.

Figure 5 shows that both the histogram threshold and the Spreen model methods yield similar sea ice classification results e from scatterometer data. MY ice was mostly in the West Weddell Sea region and FY ice was mainly in the East Weddell Sea. For the days of 31 July, 2005 and 19 August, 2005, the extent of MY ice from the histogram threshold method was 7.87×10^{5} km^2 and 11.11×10^{5} km^2, respectively. For the Spreen model method it was 6.85×10^{5} km^2 and 7.09×10^{5} km^2, respectively. The MY ice extent extracted by the histogram threshold method was slightly larger than that extracted by the Spreen model method. Figure 6 shows the difference map of sea ice classification results between histogram threshold method and Spreen model method on 31 July 2005 (Figure 6a) and 19 August 2005 (Figure 6b). The distribution of differences (histogram threshold – Spreen model) is mainly located in the west Weddell Sea.

3.3 Validation based on the ASPeCt ship-observation data

In order to compare ASPeCt ship-observation data with FY and MY ice classifications derived from QuikSCAT backscatter. The sea ice types extracted from the ASPeCt data are grouped as MY ice and FY ice. ASPeCt ship-observations record up to three fractional types of different sea ice. For our comparison, that ice stage within a subregion with the highest partial ice concentration is assumed to represent the whole subregion. The sea ice classification results of the two methods were assessed against the ASPeCt ship-observation on the same date, and are shown in Table 1. The classification accuracy using the histogram threshold method is 77.8%, while the accuracy is 80.3% for the Spreen model method. Relatively speaking, the accuracy of the Spreen model method is higher than the histogram threshold method for QuikSCAT scatterometer data.

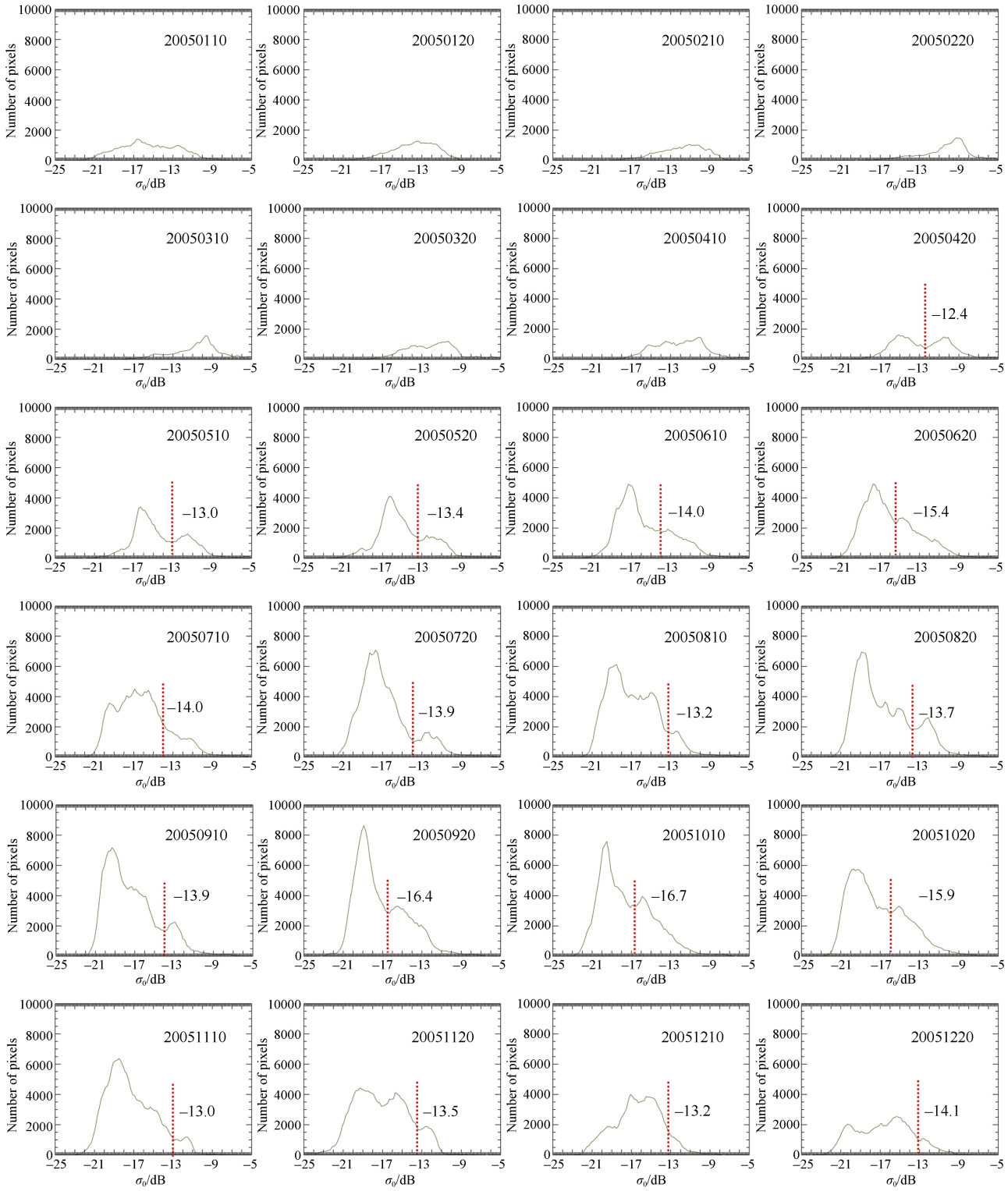

Figure 4 Histograms of QuikSCAT VV backscatter for Weddell Sea ice in 2005.

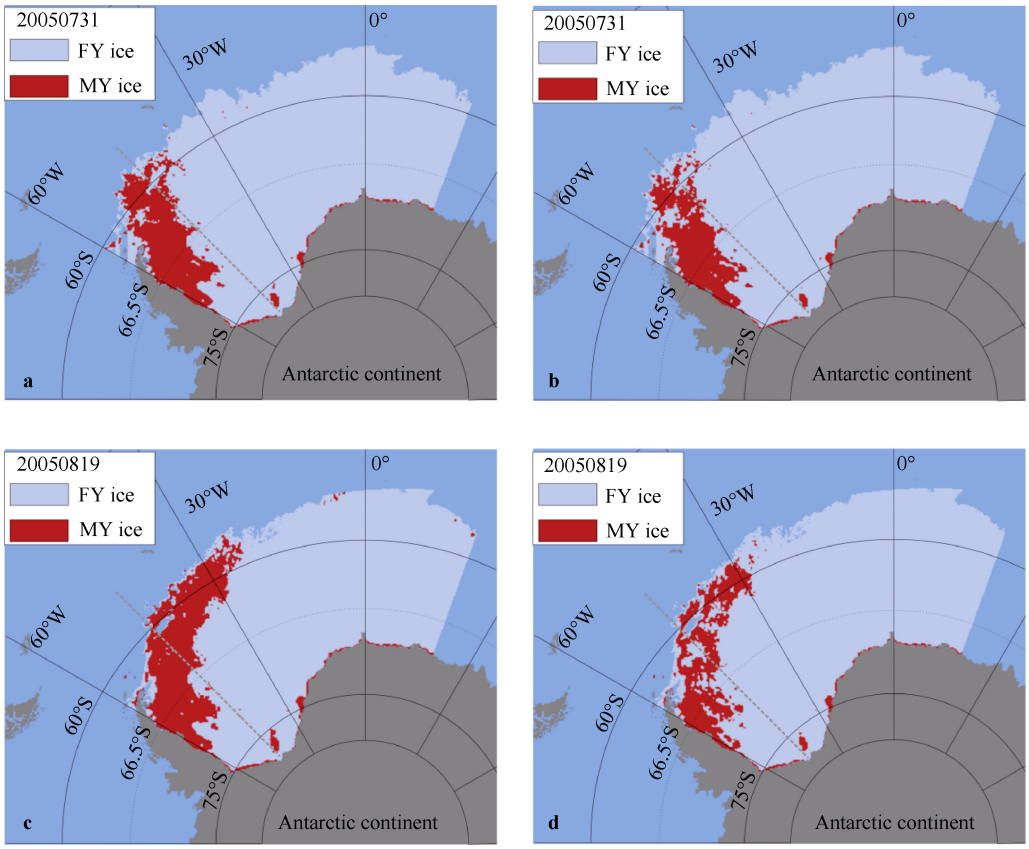

Figure 5 Comparison of sea ice type obtained by the histogram threshold and the Spreen model methods: **a** and **c** are the classification results based on the histogram threshold method, **b** and **d** are the classification results based on the Spreen model method.

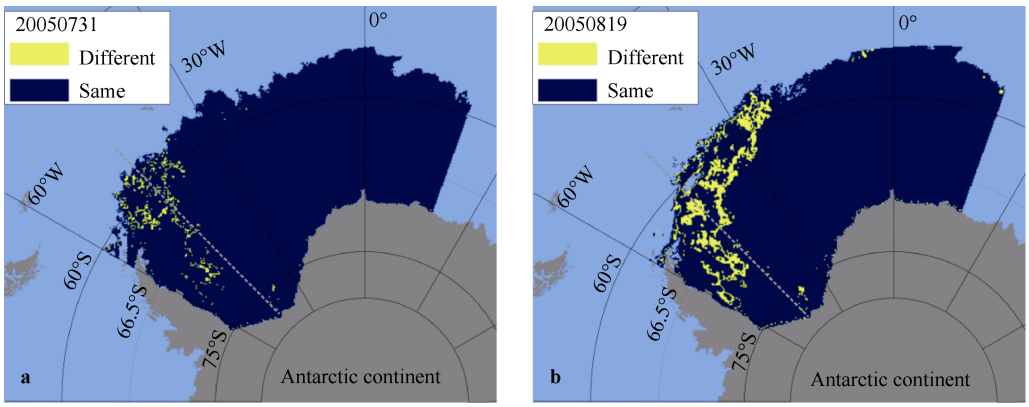

Figure 6 Map of sea ice classification differences between the histogram threshold method and the Spreen model method for 31 July 2005 (**a**) and 19 August 2005 (**b**). The yellow areas indicate a difference between the two methods, while the dark-blue areas indicate the same classification results.

4 Conclusions

Sea ice type (MY ice and FY ice) is an important parameter of sea ice, and a contentious in large-scale sea ice classification using remote sensing data. In this paper, sea ice in the Weddell Sea was classified by the histogram threshold method and the Spreen model method from QuikSCAT scatterometer data, and the classification results were evaluated against ASPeCt ship-based observational data. It is concluded that there are obvious peak-valley structures in the QuikSCAT sea-ice histogram during the sea ice growth period, so the histogram threshold method can effectively distinguish MY ice from FY ice. Both methods are suitable for classifying sea ice type using the

Table 1 Comparison of sea ice classification results between threshold method and Spreen model method using ship-based sea ice type observation data

Date	Number of ASPeCt samples	Number of consistent samples from histogram threshold method	Number of consistent samples from Spreen model method	Accuracy of histogram threshold method/%	Accuracy of Spreen model method/%
20050731	17	13	14	76.47	82.35
20050801	19	14	15	73.68	78.95
20050802	15	11	11	73.33	73.33
20050803	7	6	6	85.71	85.71
20050804	7	5	6	71.43	85.71
20050805	8	7	6	87.50	75.00
20050806	7	5	6	71.43	85.71
20050807	7	5	5	71.43	71.43
20050808	6	6	5	100.00	83.33
20050809	3	3	3	100.00	100.00
20050811	2	2	2	100.00	100.00
20050812	4	3	3	75.00	75.00
20050817	8	5	6	62.50	75.00
20050818	3	3	3	100.00	100.00
20050819	4	3	3	75.00	75.00
Sum/Average	117	91	94	77.78	80.34

scatterometer data but, from the comparison with ship observations, the Spreen model method is more accurate than the histogram threshold method. This comparison of sea ice classification methods can provide a reference for obtaining long-time series of sea ice type information for the whole Antarctic. Due to the limited ship-observation data, cross-validation of multi-source data should be considered for future work, and further study should also be made on sea ice type classification from scatterometer data during the sea ice melt season.

Acknowledgments The authors would like to thank the Brigham Young University, the Bremen University and the Australian Antarctic Data Center for providing QuikSCAT, AMSR-E and ASPeCt data. The authors acknowledge the supports from the National Natural Science Foundation of China (Grant nos. 41606215 and 41576188), the National Key Research and Development Program of China (Grant no. 2017YFA0603104), the fund of SOA Key Laboratory for Polar Science (Grant no. PS1502), the fund of Key Laboratory of Global Change and Marine-Atmospheric Chemistry, SOA (Grant no. GCMAC1504), the Fundamental Research Funds for the Central Universities (Grant no. 2042016kf0038) and the Chinese Postdoctoral Science Foundation Funded Project (Grant no. 2016M602342). Comments from the anonymous referees and the editor are also gratefully appreciated.

References

Andreas E L, Lange M A, Ackley S F, et al. 1993. Roughness of Weddell Sea ice and estimates of the air-ice drag coefficient. J Geophys Res, 98(C7): 12439–12452

Beckers J F, Renner A H H, Spreen G, et al. 2015. Sea-ice surface roughness estimates from airborne laser scanner and laser altimeter observations in Fram Strait and north of Svalbard. Ann Glaciol, 56(69): 235–244

Early D S, Long D G. 2001. Image reconstruction and enhanced resolution imaging from irregular samples. IEEE Trans Geosci Remote Sens, 39(2): 291–302

Geldsetzer T, Yackel J J. 2009. Sea ice type and open water discrimination using dual co-polarized C-band SAR. Can J Remote Sens, 35(1): 73–84

Gloersen P, Cavalieri D J. 1986. Reduction of weather effects in the calculation of sea ice concentration from microwave radiances. J Geophys Res, 91(C3): 3913–3919

Haarpaintner J, Spreen G. 2007. Use of enhanced-resolution QuikSCAT/SeaWinds data for operational ice services and climate research: sea ice edge, type, concentration, and drift. IEEE Trans Geosci Remote Sens, 45(10): 3131–3137

Heygster G, Wang H. 2010. Remote sensing of multiyear sea ice using AMSR-E 89 GHz data//38th COSPAR scientific assembly. Bremen: Cospar Scientific Assembly, 38

Kawanishi T, Sezai T, Ito Y, et al. 2003. The Advanced Microwave Scanning Radiometer for the Earth Observing System (AMSR-E), NASDA's contribution to the EOS for global energy and water cycle studies. IEEE Trans Geosci Remote Sens, 41(2): 184–194

Kwok R. 1998. The RADARSAT geophysical processor system// Tsatsoulis C, Kwok R. Analysis of SAR data of the Polar Oceans: recent advances. Berlin Heidelberg: Springer, 235–257

Kwok R. 2004. Annual cycles of multiyear sea ice coverage of the Arctic Ocean: 1999–2003. J Geophys Res, 109(C11): C11004

Long D G, Hardin P J, Whiting P T. 1993. Resolution enhancement of spaceborne scatterometer data. IEEE Trans Geosci Remote Sens, 31(3): 700–715

Lythe M, Hauser A, Wendler G. 1999. Classification of sea ice types in the Ross Sea, Antarctica from SAR and AVHRR imagery. Int J Remote Sens, 20(15–16): 3073–3085

Ma L J, Lu L H, Bian L G. 2004. Spatio-temporal character of Antarctic sea ice variation. Chin J Polar Res, 16(1): 29–37

Maslanik J, Stroeve J, Fowler C, et al. 2011. Distribution and trends in Arctic sea ice age through spring 2011. Geophys Res Lett, 38(13): L13502

NASA/JPL. 2006. QuikSCAT science data product—user's manual. America: California Institute of Technology

Ozsoy-Cicek B, Kern S, Ackley S F, et al. 2011. Intercomparisons of Antarctic sea ice types from visual ship, RADARSAT-1 SAR, Envisat ASAR, QuikSCAT, and AMSR-E satellite observations in the Bellingshausen Sea. Deep Sea Res Part II Top Stud Oceanogr, 58(9–10): 1092–1111

Spreen G. 2008. Satellite-based estimates of sea ice volume flux: applications to the Fram Strait region. Ph.D. thesis, Hamburg: Hamburg University

Thorndike A S, Rothrock D A, Maykut G A, et al. 1975. The thickness distribution of sea ice. J Geophys Res, 80: 4501–4513

Tucker III W B, Grenfell T C, Onstott R G, et al. 1991. Microwave and physical properties of sea ice in the winter marginal ice zone. J Geophys Res, 96(C3): 4573–4587

Vancoppenolle M, Fichefet T, Goosse H, et al. 2009. Simulating the mass balance and salinity of Arctic and Antarctic sea ice. 1. Model description and validation. Ocean Model, 27(1–2): 33–53

Walker N P, Partington K C, Van Woert M L, et al. 2006. Arctic Sea Ice type and concentration mapping using passive and active microwave sensors. IEEE Trans Geosci Remote Sens, 44(12): 3574–3584

Worby A P, Geiger C A, Paget M J, et al. 2008. Thickness distribution of Antarctic sea ice. J Geophys Res, 113(C5): C05S92

Zwally H J, Comiso J C, Parkinson C L, et al. 2002. Variability of Antarctic sea ice 1979–1998. J Geophys Res, 107(C5): 9-1–9-19